Polymer Science, Ser. C, Vol. 44, No. 1, 2002, pp. 83–99. Translated from Vysokomolekulyarnye Soedineniya, Ser. C, Vol. 44, No. 9, 2002, pp. 1701–1719.

Structure and Properties of Low-Molecular-Mass Substances in Solvent-Crazed Polymer Matrices[1]

A. L. Volynskii[2], O. V. Arzhakova, L. M. Yarysheva, and N. F. Bakeev

Faculty of Chemistry, Moscow State University, Leninskie gory, Moscow, 119899 Russia

Abstract—The literature data on the mechanism of structural rearrangements in solid polymers (films and fibers) upon solvent crazing in the presence of liquid media are reviewed. The collected experimental evidence allows one to consider solvent crazing as a specific mode of spontaneous polymer dispersion into fine aggregates of disperse macromolecules upon joint action of mechanical stress and an active liquid medium and as a means of colloidal dispersion of low-molecular-mass compounds in a polymer matrix. As is shown, the phenomenon of solvent crazing offers new routes to the preparation of various nanocomposites based on various glassy and semicrystalline polymers containing target additives of almost any low-molecular-mass compound. Some aspects of the practical application of solvent crazing as an efficient method for the modification of polymer films and fibers are discussed.

INTRODUCTION

Solvent crazing of polymers constitutes a certain mode of plastic deformation of solid polymers [1]. This deformation presents a specific manifestation of the Rehbinder phenomenon in polymers [2] and leads to the dispersion of a solid polymer into the fine aggregates composed of oriented macromolecules (craze fibrils) which are separated by the pores of similar dimensions. It is important to note that the dimensions of craze fibrils and microvoids between them are equal to ~1–100 nm; that is, their dimensions correspond to the dimensions of phases which are characteristic of nanocomposites. The development of a stable fibrillar–porous structure via solvent crazing is possible only when the as-formed micropores are filled with the surrounding liquid medium in which the deformation of a polymer is carried out. As a result, both the polymer and low-molecular-mass compound, which is thermodynamically incompatible with the polymer, appear to be not only mutually dispersed down to a nanometric level but also form a highly disperse and highly homogeneous mixture.

In this connection, we will discuss in detail some problems related to the development of the porous structure in polymers and possible introduction of various low-molecular-mass compounds into the polymer structure via solvent crazing, as well as various specific phenomena, which are related to the interaction of incorporated low-molecular-mass compounds with the porous polymer matrix. An appreciable part of this review is devoted to the structure and properties of low-molecular-mass compounds involved in the porous structure of solvent-crazed polymers, as well as to some applied aspects of the phenomenon of solvent crazing in polymers.

SPECIFIC FEATURES OF SOLVENT CRAZING FOR THE DEVELOPMENT OF POROSITY IN POLYMERS

As was mentioned above, inelastic deformation of polymers in the presence of physically active liquid media proceeds via the mechanism of solvent crazing [1]. Physically active liquids do not provide any bulk swelling (dissolution) of the unstressed polymer but should easily wet it, that is, should reduce its surface energy. Such liquids are referred to as adsorptionally active media (AAM) [3]. When the tensile stress is applied to a sample in the presence of AAM, the stress-induced development of the specific zones of a plastically deformed porous fibrillar material referred to as crazes takes place. Due to the existence of a well-defined boundary between the undeformed polymer and as-nucleated crazes, the whole process may be easily detected and studied by direct microscopic observations [1]. Comprehensive microscopic studies allowed one to reveal the multistage character of solvent crazing and to ascertain its correlation with the mechanical response of the deformed polymer [4].

Figure 1 schematically represents the general stages of the development of solvent crazing in polymers in the presence of a liquid medium. As is seen, at the early stages of the tensile drawing of the polymer, a certain number of crazes is nucleated on the polymer surface (the stage of craze nucleation).

[1] This work was supported by the Russian Foundation for Basic Research, project no. 99-03-33459a, the Program "Universities of Russia," project no. 015060206, and the NWO Foundation (The Netherlands).
[2] E-mail: volynskii@mail.ru

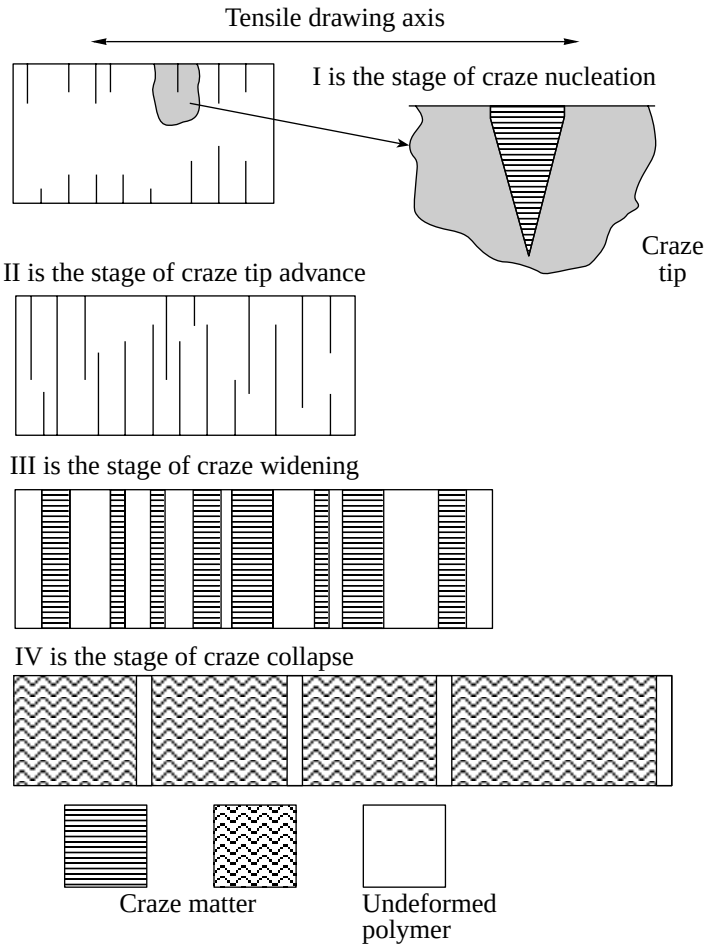

Fig. 1. Schematic representation of various stages of solvent crazing in polymers: I is the stage of craze nucleation, II is stage of craze tip advance, III is the stage of craze widening (thickening), and IV is the stage of craze collapse.

Upon a further tensile drawing, the nucleated crazes propagate in the direction perpendicular to the direction of tensile drawing, and the width of the growing crazes is almost constant and rather small (fractions of micron) (the stage of craze tip advance). This process proceeds until individual growing crazes or their ensemble cross the whole cross section of the sample. Then, the next stage of solvent crazing commences when the as-grown crazes begin to increase their dimensions along the direction of tensile drawing (the stage of craze thickening or craze widening). Evidently, at this stage, the principal transformation of the polymer to the oriented (fibrillar) nanoporous state takes place.

Upon the solvent crazing of polymers in the presence of AAM, another stage exists: when most of the polymer is transformed into an oriented fibrillar state, the collapse of the as-formed porous structure takes place [5]. This final stage of solvent crazing is accompanied by a dramatic side contraction of the deformed polymer which leads to a concomitant decrease in porosity [6], mean pore dimensions [7], and specific surface [1]. The mechanism of collapse has been discussed at length in [8]: as was shown, this stage of solvent crazing is controlled by the natural draw ratio of polymer, as well as by the properties of AAM and geometry of the deformed sample.

All stages of solvent crazing are accompanied by the development and evolution of the microscopic porosity in the solvent-crazed polymer. The whole process was described in more detail in [9]; here, we will only present the typical dependence of porosity on the tensile strain of the solvent-crazed polymer (Fig. 2). As follows from Fig. 2, at the early stages of tensile drawing, the volume porosity increases, and this increase is related to the nucleation and further growth of crazes. However, at relatively high tensile strains, the above-mentioned collapse of the porous structure of the polymer takes place; this process is accompanied by a decrease in the total porosity of the sample. As a result, the dependence of the porosity on tensile strain passes a maximum.

PROPERTIES OF THE SOLVENT-CRAZED POLYMER MATRIX–LIQUID LOW-MOLECULAR-MASS COMPONENT SYSTEMS

Hence, a highly disperse polymer matrix with pores filled with a surrounding liquid may be prepared in the

simplest way (by the tensile drawing of polymer samples in the presence of AAM). When the sample is removed from AAM, and the low-molecular-mass liquid is allowed to evaporate from the volume of crazes (in this case, the sample is kept either in a free state or under isometric conditions), various crucial phenomena take place; the above behavior is provided by the coagulation of a highly disperse fibrillar material of crazes [10–13]. It is necessary to note that, in this case, evaporation of even high-volatile liquids is retarded due to the specific features of the structural organization of the solvent-crazed material. Under such conditions, the evaporation of the low-molecular-mass component may last over many weeks [14]. The above phenomena are especially interesting for the solvent-crazed samples with high tensile strains as achieved upon the tensile drawing of polymer in the presence of AAM when the collapse of the porous structure in crazes occurs. As a result of the collapse, a certain amount of the liquid appears to be efficiently encapsulated in the polymer structure. Therefore, the liquid low-molecular-mass component appears to be preserved in the polymer structure, and the resultant material is characterized by quite unusual mechanical properties [14].

When the solvent-crazed sample is loaded with a viscous nonvolatile liquid, even more fascinating phenomena are observed [15, 16]. Figure 3 shows the weight loss curves for PET samples containing a nonvolatile liquid component (glycerol) which was introduced into the polymer structure via solvent crazing. As is seen, in this case, the collapse of the craze structure and the concomitant phenomenon of syneresis span over many months and even years. The rate of this process is controlled, in particular, by the nature of the liquid component and polymer, the geometry of the test sample, and the conditions of tensile drawing. It is important to mention that, in the case studied, we deal with highly disperse blends of a polymer and an incompatible low-molecular-mass liquid. It is this incompatibility that is responsible for the phase separation in such systems. The slow rates of the above processes may be explained by the fact that the diameter of microvoids in the polymer structure is so small that it appears to be comparable to the molecular dimensions of the introduced low-molecular-mass liquid. As a result, a certain fraction of the nonvolatile low-molecular-mass component, which was introduced into the polymer structure via solvent crazing, may be preserved in the polymer for an indefinitely long period of time. Actually, this implies that the solvent crazing of polymers may be treated as a certain mode of microencapsulation of low-molecular-mass liquid components in the polymer films and fibers. Note that “encapsulation” of the liquid low-molecular-mass component in the incompatible polymer matrix presents a challenging scientific and applied task [17].

SOME APPROACHES TO PREPARATION OF NANOCOMPOSITES BASED ON SOLVENT-CRAZED POLYMER MATRICES AND THEIR CHARACTERISTICS

An important feature of solvent crazing concerns the fact that micropores formed in the structure of a growing craze are efficiently filled with the surrounding liquid medium. In turn, the introduction of the low-molecular-mass component into the nanoporous craze structure is accompanied by its dispersion down to the colloidal dimensions. As a result, solvent crazing allows one to achieve a high level of mutual dispersion and to prepare highly homogeneous polymer blends containing the incompatible low- or high-molecular-mass component. As the dimensions of craze fibrils and micropores between them are equal to ~1–100 nm, one may conclude that they correspond to phase dimensions which are characteristic of nanocomposites. In this connection and taking into account the specific fibrillar–porous structure of the solvent-crazed polymer, poly-

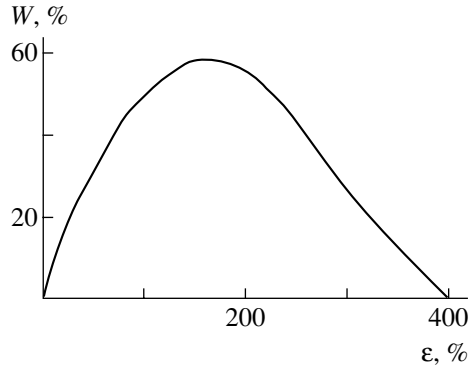

Fig. 2. Porosity vs. tensile strain upon the tensile drawing of PET in AAM.

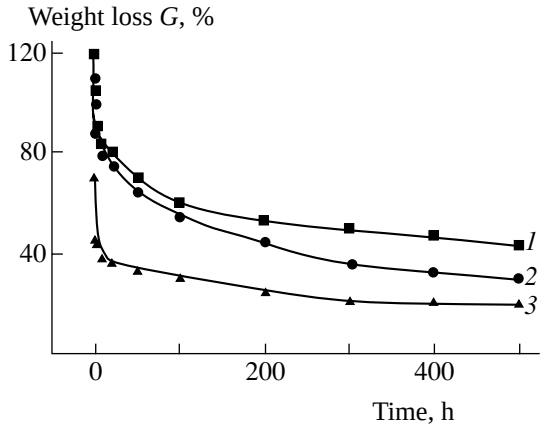

Fig. 3. The time dependence of weight loss for the solvent-crazed PET samples containing glycerol (the tensile drawing of initial PET fibers was performed in 25% alcohol solution in glycerol). Tensile strain: (*1*) 100, (*2*) 200, and (*3*) 300%.

mer blends based on such microporous polymer matrices containing low-molecular-mass substances may be classified into a special class of nanocomposites.

Therefore, the tensile drawing of the polymer in the presence of an appropriate liquid medium via solvent crazing makes it possible to deliver the thermodynamically incompatible low-molecular-mass component to the polymer and to provide its dispersion down to the colloidal dimensions.

Note that the approach of solvent crazing enables the introduction of almost any low-molecular-mass compounds into the polymer structure. The tensile drawing of polymers in the presence of a liquid, which serves as a target additive by itself (a low melting temperature of the low-molecular-mass component), or in an AAM solution containing the dissolved target low-molecular-mass component, provides the only necessary condition. In the first case, the low-molecular-mass compound serves by itself as AAM at elevated temperatures (however, evidently, at temperatures below the glass transition temperature or the melting temperature of the deformed polymer). As a result, the tensile drawing of the polymer in the melt of this compound proceeds via the mechanism of solvent crazing, and the as-formed porous structure appears to be filled with this substance. Upon a further cooling, in situ crystallization of the low-molecular-mass component takes place, and the polymer nanocomposite, in which the low-molecular-mass component is crystallized in its highly disperse state, is obtained.

In the second case, the solution of the target additive in AAM is introduced into the volume of crazes. Upon further evaporation of the volatile component, in situ crystallization of the dissolved target component in the pores of the solvent-crazed polymer proceeds. Evidently, the volume of crazes may be filled with the low-molecular-mass substances with almost any melting temperatures [18, 19].

Both methods involve the direct introduction of the low-molecular-mass compounds into the volume of crazes; therefore, hereinafter, this mode of introduction is referred to as *direct method.*

Obviously, there are many substances that may hardly be introduced into the solvent-crazed polymer via the above procedure. For example, one may mention metals, many metal salts, metal oxides, and other inorganic compounds. In this case, the polymer–low-molecular-mass compound systems may be prepared via the corresponding chemical reactions of precursors directly in the porous structure of crazes (in situ reaction). Hereinafter, this method of preparing polymer nanocomposites will be referred to as indirect method of the introduction of low-molecular-mass compounds into the structure of crazes.

Direct Method of the Preparation of Highly Disperse Blends via Solvent Crazing of Polymers

The pioneering studies on the introduction of low-melting compounds into the polymer structure via solvent crazing were performed for the system composed of an amorphous PET and *n*-octadecane (OD) (T_m = 28°C) [20]. The polymer sample was stretched in the presence of a liquid OD at 50°C and cooled in the hand-operating clamps. As a result, the porous structure of crazes was filled with OD, which is an efficient AAM, and, upon a further cooling, its subsequent crystallization in the polymer matrix took place. This simple approach enabled nanocomposites containing up to 50 wt % and more of the low-molecular-mass component to be prepared. The amount of the introduced low-molecular-mass component would be controlled by the level of the volume porosity and would depend on the evolution of the polymer porous structure upon its tensile drawing in AAM (Fig. 1). Independently of the tensile strain of polymer samples upon solvent crazing, the low-molecular-mass component appears to be dispersed to fine aggregates, and the dimensions of such aggregates are comparable to the dimensions of pores in the craze structure (tens–hundreds of angstroms). The preparation of the above nanocomposites not only offers new routes to develop a new class of promising advanced materials based on the solvent-crazed polymers but also provides an efficient means to characterize the properties of components in their highly disperse colloidal state. Let us consider the results of such studies.

The specific features of phase transitions of low-molecular-mass compounds in the volume of crazes. The DSC method offers a tool of obtaining information concerning the state of low-molecular-mass compounds in the narrow pores. Figure 4 presents the typical DSC curves for the crystallization of OD in a free state and in the porous structure of PET. As follows from the DSC scans, the crystallization of the hydrocarbon in its free state is seen at 24°C; this process manifests itself as a nonsymmetric endothermic peak. The latter observation is likely to be related to a transition from a rhombic to hexagonal packing which takes place in the temperature region of melting; this behavior is typical of saturated hydrocarbons [21]. At the same time, OD incorporated into the solvent-crazed polymer matrix shows some earlier unknown specific features in its thermophysical properties. As is seen in Fig. 4 (curve *b*), the crystallization appears to proceed via two stages. First, one may observe the transition which takes place at a temperature corresponding to the transition in the free-standing OD; then, one may detect an exothermic peak at a temperature that is 6–8°C lower than the melting temperature of the free OD. As is well seen, the principal contribution (~80%) to the heat of crystallization is provided by a wide low-temperature peak.

The reasons for the above difference may be explained when studying the removal of OD from the porous structure of the solvent-crazed PET sample by rinsing. Figure 5 presents relative changes in the weight (weight loss) of the OD-containing PET sample plotted against the time of its treatment with *n*-hexane. As is well seen, most of the introduced OD may be actually washed out from the structure; however, a marked fraction of OD is still preserved in the polymer. Figure 6 shows the DSC curves for the crystallization of OD in the PET samples after their treatment with *n*-hexane for different periods of time. As is seen, the first fraction, which is removed from the sample, is the fraction of OD whose crystallization temperature coincides with the crystallization temperature of the free-standing OD (Fig. 6, curves *1* and *2*). Upon a further rinsing, a gradual removal of the fraction of OD, which provides the low-temperature wide crystallization peak, is seen (curves *2*–*7*). Even though, upon a prolong rinsing, all temperature transitions in the PET–OD system are faded, and the corresponding X-ray reflections in X-ray patterns disappear, a marked fraction of OD is still preserved in the polymer sample (Fig. 5).

Evidently, the high-temperature crystallization peak is provided by a certain low amount of OD which is located on the surface of the sample in macroscopic relief grooves or in large pores. Naturally, thermophysical characteristics of this fraction of OD are virtually similar to those of the free-standing OD (cf. Figs. 4 (curve *a*) and 6). A wide low-temperature crystallization peak is likely to be related to the fraction of OD, which is incorporated into the porous structure of crazes. The above decrease in the crystallization temperature is provided by changes in the transition temperature which depend on the dimensions of the as-formed crystallization nucleation centers. According to the formal theory of crystallization nucleation, the smaller the nucleation center or the length of the region of a new phase, the lower the corresponding crystallization temperature. By the value of supercooling, one may assess the size of the characteristic nucleation center upon crystallization of the free-standing OD. This value was estimated from the DSC data to be equal to ~165 Å; that is, this value is comparable to the pore dimensions in crazes.

Therefore, the size of the nucleation center is much higher than the effective size of the most pores in the structure of the solvent-crazed PET. The dimensions of the crystallizing phase are limited by pore walls, and its length appears to be smaller than the size of the nucleation center in the free OD. As a result, the crystallization of the substance being dispersed to such small aggregates takes place at much lower temperatures. Taking into account the fact that the pore size distribution of the solvent-crazed polymers is rather wide, the low-temperature crystallization peak appears to be rather extended along the temperature axis. This observation allows the above phenomenon to be applied for the analysis of typical pore size distributions in the solvent-crazed polymer as prepared by the tensile drawing in the presence of a given AAM. The related calculation procedure was presented in [20]. Figure 7 presents the results of the above calculation as pore size distributions for the solvent-crazed PET samples, which were

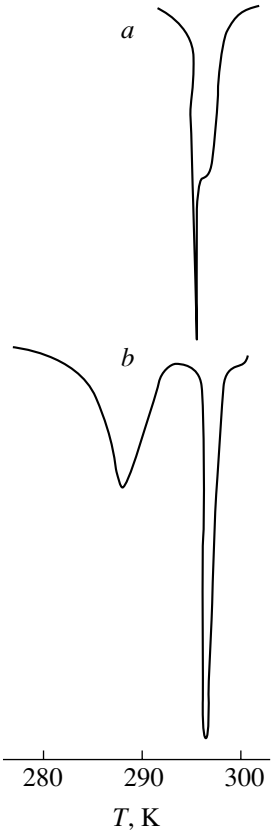

Fig. 4. The DSC curves for crystallization of (*a*) free-standing OD and (*b*) OD in the crazes of PET. The tensile strain of OD-containing PET is 50%.

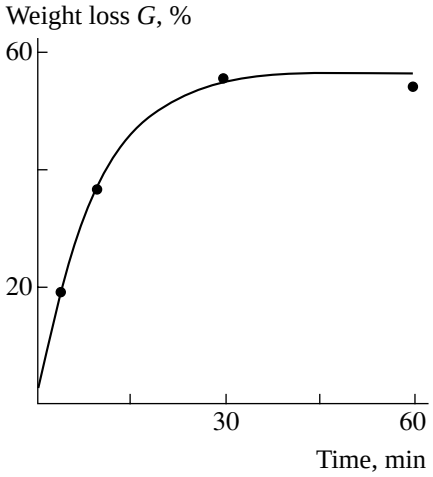

Fig. 5. Weight loss in the OD-containing solvent-crazed PET sample vs. the duration of treatment with *n*-hexane.

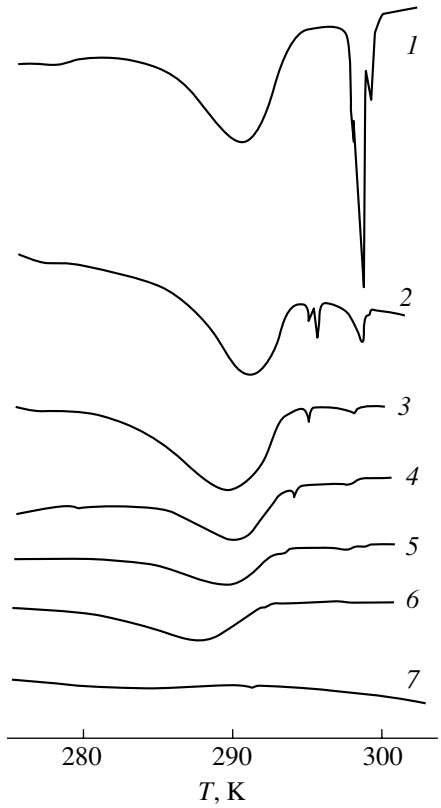

Fig. 6. DSC curves for OD-containing PET samples after their washing with *n*-hexane for (*1*) 0, (*2*) 5, (*3*) 10, (*4*) 15, (*5*) 20, (*6*) 30, and (*7*) 60 min.

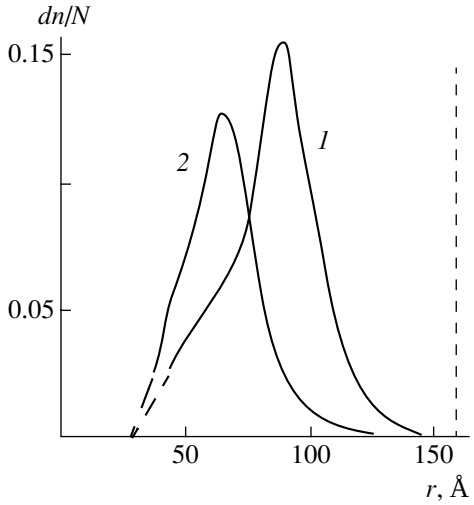

Fig. 7. Pore size distribution curves for the solvent-crazed PET samples obtained by tensile drawing in OD to a tensile strain of (*1*) 50 and (*2*) 400%. Extrapolation to the x-axis gives the size of the critical nucleation center for the crystallization of OD in free state.

prepared by the tensile drawing in the presence of OD to a tensile strain of 50 or 400%. As is seen, as the tensile strain is increased, one may observe a marked decrease in the effective pore diameter which may be estimated from the depression in the crystallization temperature. This result agrees with the above speculations concerning the evolution of the porous structure in the polymer upon its tensile drawing in the presence of AAM (Figs. 2 and 3).

However, it seems evident that the above pore size distributions may hardly provide a detailed and adequate description of the porous structure of the solvent-crazed polymer. As follows from Figs. 5 and 6, when, as a result of rinsing, the thermal transitions and corresponding X-ray reflections are faded out, the sample still contains quite appreciable amounts of residual OD. As was shown in [20], the fraction of the unwashed OD increases with increasing the tensile strain of the solvent-crazed sample and achieves rather high values (~25 wt %). The above evidence suggests that the solvent-crazed polymer with high tensile strains contains appreciable amounts of inner microvoids which are inaccessible for the solvent; therefore, the incorporated low-molecular-mass compound cannot be completely removed from the polymer via solvent extraction. This specific structure is produced via the structural collapse in crazes as is shown in Fig. 1. At the same time, the above closed microvoids appear to be so small that the encapsulated OD may hardly form a continuous crystalline phase; as a result, the corresponding DSC scans show no phase transitions. The corresponding X-ray patterns also show no X-ray reflections which are typical of the crystalline structure of OD. In other words, a certain fraction of the low-molecular-mass component is located in the pores with so small dimensions that the development of a continuous crystalline phase is impossible. Therefore, this offers an interesting opportunity to assess the size of structural molecular aggregates below which the thermodynamic term *phase* becomes incorrect. As follows from Fig. 7, for OD, this size is equal to ~25 Å.

Hence, the introduction of low-molecular-mass organic compounds into the polymer stretched in the presence of AAM allows one to gain additional information concerning its porous structure. Taking into account the fact that the low-molecular-mass component is dispersed to the fine aggregates (tens of aggregates) in the polymer matrix, this offers an experimental opportunity to investigate the specific features of phase transitions in highly disperse systems.

As was shown in subsequent studies, the above specific features of the phase transitions of low-molecular-mass compounds in solvent-crazed polymer matrices show a general character. These features (widening in phase transitions and shift to a low-temperature region) are observed for various low-molecular-mass compounds (hydrocarbons, fatty acids, and alcohols) and for various solvent-crazed polymers (PET, HDPE, PP, PA, PTFE, PMMA, PVC) [22–28]. Evidently, this general character of the above phenomena is related to the features of the fibrillar–porous structure of crazes. Let us mention that the above behavior is reported for the

solvent-crazed polymers prepared via the mechanism of both classical and delocalized solvent crazing [1]. This is due to the fact that, in this case, the effective pore dimensions, rather than the morphological organization of the as-formed porous structure, play the key role. For both modes of solvent crazing, the characteristic pore dimensions are equal to 10–200 Å; that is, they correspond to the region of typical colloidal dimensions. This fact is responsible for the principal features of the phase transitions of low-molecular-mass compounds in such systems.

In addition to the above-mentioned thermophysical behavior of low-molecular-mass compounds in the craze structure, let us discuss the following aspects. For the compounds which are capable of polymorphic transitions, their crystallization in narrow pores is characterized by their own specific features. For example, the phase composition of low-molecular-mass compounds involved in porous polymer matrices was studied by the DSC method [25, 27]. Figure 8 presents the DSC curves for a normal hydrocarbon, heneicosane (HE), in a free state and in the crazes of various polymer matrices. The appearance of two peaks in the DSC scans (curve *1*) is related to the polymorphic transition in the free-standing HE from the *R*- to *A*-modification. Curves *2–4* show a single wide high-temperature peak which corresponds to the melting of HE in crazes. Therefore, one may conclude that, in the crazes of various polymer matrices, HE exists only in the *R*-modification. Similar results concerning the existence of the high-temperature modification of the low-molecular-mass compound in crazes have been obtained for tridecoic acid (TDA) and cetyl alcohol (CA) [25, 27]. In all cases, the incorporated component involved in the porous polymer structure exists in its high-temperature modification, which appears to be unstable for the same compound, but in its free state at room temperature.

A high stability of modifications of the low-molecular-mass compounds, which are unstable in their free state, may be rationalized by taking into account a high level of dispersion in the microporous structures. In micropores, all polymorphic transitions may take place only in the temperature interval where the radius of the critical nucleation center of the low-temperature phase is lower or equal to the pore radius. When the temperature at which this condition is fulfilled does not lie within the temperature interval wherein the rate of formation of a new phase is rather high, no polymorphic transitions take place and only the high-temperature polymorphic modification of the low-molecular-mass compound is formed.

As was shown above, the low-molecular-mass compounds crystallized in the micropores of solvent-crazed oriented polymer matrices exist in a highly disperse state. Therefore, the analysis of their phase transitions should be conducted taking into account the surface component of the corresponding thermodynamic potentials (free energy, enthalpy, entropy). Let us present the thermodynamic potentials of the low-molecular-mass compound as the sum of volume and surface components. Then, taking into account the fact that, upon the polymorphic transition, the specific surface of the system remains unchanged, one may derive equations which describe variations in specific surface components of the thermodynamic potential at the polymer–low-molecular-mass compound boundary, as well as the dependences of the thermodynamic parameters of the melting process of the low-molecular-mass compound on the size of the critical nucleation center (the size of limiting pores).

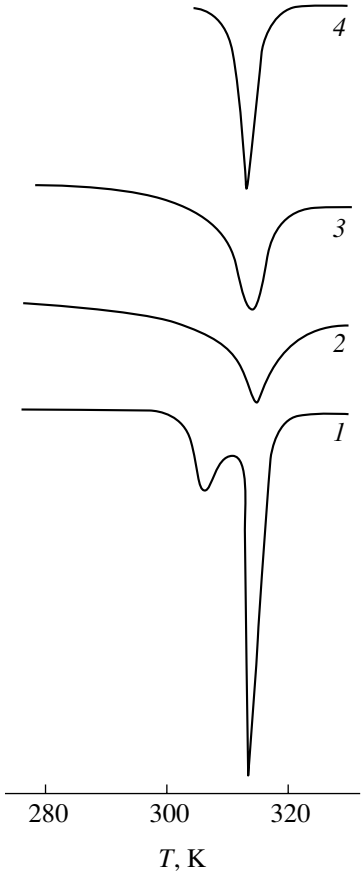

Fig. 8. DSC melting curves of HE in (*1*) the free state and in the solvent-crazed samples of (*2*) HDPE, (*3*) PA-6, and (*4*) PET.

It is important to mention that the pore dimensions in the polymer structure control not only the process of melting of the low-molecular-mass compound but also its crystallization in the porous polymer matrix. This fact has been convincingly proved when studying the processes of melting and crystallization of TDA in the crazes of the solvent-crazed PET samples by the DSC method (Fig. 9). Crystallization of the low-molecular-mass component in the micropores of the solvent-crazed polymer proceeds at temperatures when the radius of the critical nucleation center becomes equal to the pore radius.

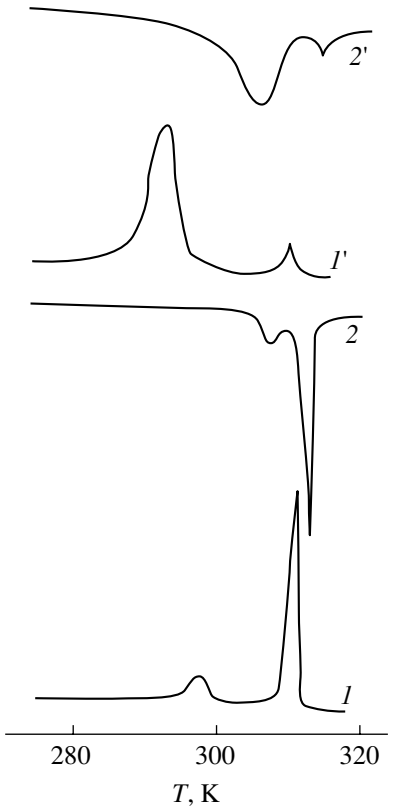

Fig. 9. DSC curves for (*1*, *1*') crystallization and (*2*, *2*') melting of TDA (*1*, *2*) in free state and (*1*', *2*') in the crazes of PET.

In this case, one may also estimate the sizes of the critical nucleation center from the experimental thermodynamic parameters of the phase transition of the low-molecular-mass compound in polymer matrices and in the free state.

To verify the applicability of the advanced thermodynamic approach to the description of the phase transitions of low-molecular-mass compounds in the porous structure of polymer matrices, the parameters of the solvent-crazed structure (the dimensions of craze pores and fibrils) were estimated by the method of small-angle X-ray scattering. Table 1 presents the comparison of the above results with the corresponding DSC data [28, 29]. A fair agreement between the values obtained by various methods is achieved, and this fact provides a convincing evidence for the applicability of the thermodynamic analysis to the description of phase transitions of low-molecular-mass components in the crazes of polymers.

Table 1. Parameters of the porous structure of solvent-crazed polymers

System	Diameter of craze fibrils, nm	Pore diameter, nm
PET–HE	8.0	6.0/6.5
PET–TDA	10.5	7.0/5.0
PC–TDA	29.0	7.0/5.0
PA-6–CA	8.3	4.6/7.0

Note: Numerator and denumerator presents the data of SAXS and pressure-driven liquid permeability, respectively.

Hence, the introduction of the low-molecular-mass substances into the porous structure of solvent-crazed polymers is accompanied by their transformation into a highly disperse state. Upon transition of the low-molecular-mass compounds to the highly disperse state, the character of their phase transitions in such systems is markedly changed. The analysis of phase transitions of the low-molecular-mass compounds in the polymer matrices and in the free state illustrates a marked effect of the porous structure of polymers on their thermal behavior and enables one to gain knowledge of the structure of pores in the volume of crazes, as well as of the state of the low-molecular-mass component in narrow pores.

Orientational phenomena upon the crystallization of low-molecular-mass compounds in the volume of crazes. The above-described thermal properties of low-molecular-mass compounds introduced into the structure of crazes are related to the specific features of their crystallization in narrow pores (1–30 nm). Such small dimensions of pores are not the only feature of the structural organization of crazes. The parallel arrangement of craze fibrils in the craze structure along the direction of the tensile drawing appears to be rather important (Fig. 1). This implies that the narrow asymmetric pores separating the individual craze fibrils also appear to be mutually oriented along the direction of the tensile drawing of the polymer. A well-pronounced asymmetry of the craze structure should also exert a certain effect on the crystallization of low-molecular-mass compounds in the craze volume.

This effect was revealed and characterized when solvent-crazed polymer–low-molecular-mass component systems were studied by X-ray analysis [18, 19, 29]. As was found, independently of the polymer matrix and the nature of the incorporated crystallizable component, the crystallization of the low-molecular-mass component is accompanied by the formation of highly ordered structures. Figure 10 illustrates this phenomenon for the solvent-crazed PET containing various low-molecular-mass compounds. As is well seen, the crystallization of the above substances leads to the development of highly ordered structures, and the corresponding X-ray patterns appear to be similar to the X-ray patterns characteristic of single crystals.

The above phenomenon shows a general character and is observed when crystallizable (PET, PC) and amorphous polymers (atactic PMMA) are used as polymer matrices [18, 19]. All the above features are pre-

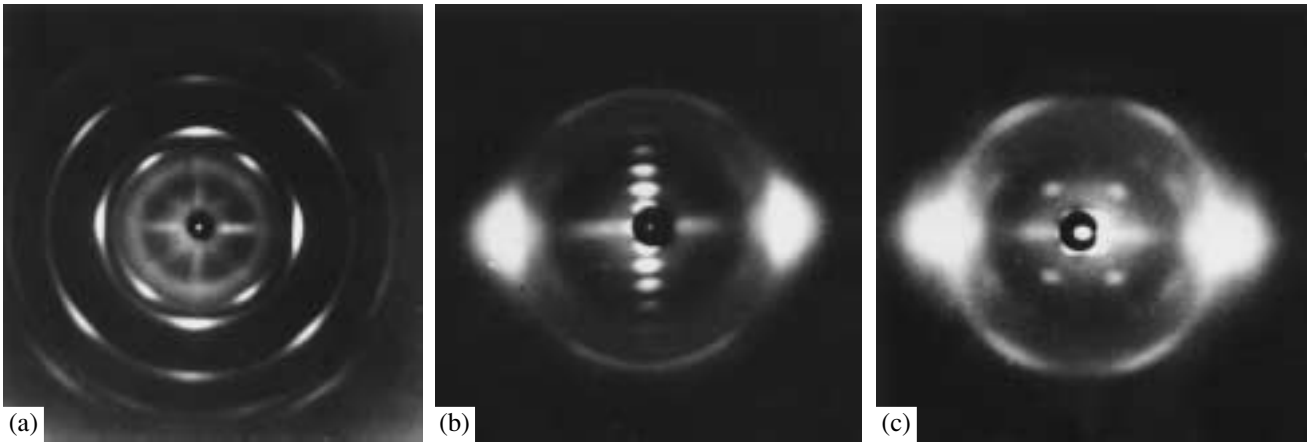

Fig. 10. X-ray patterns of the solvent-crazed PET samples containing (a) KI and (b) OD and (c) solvent-crazed PC sample containing TDA.

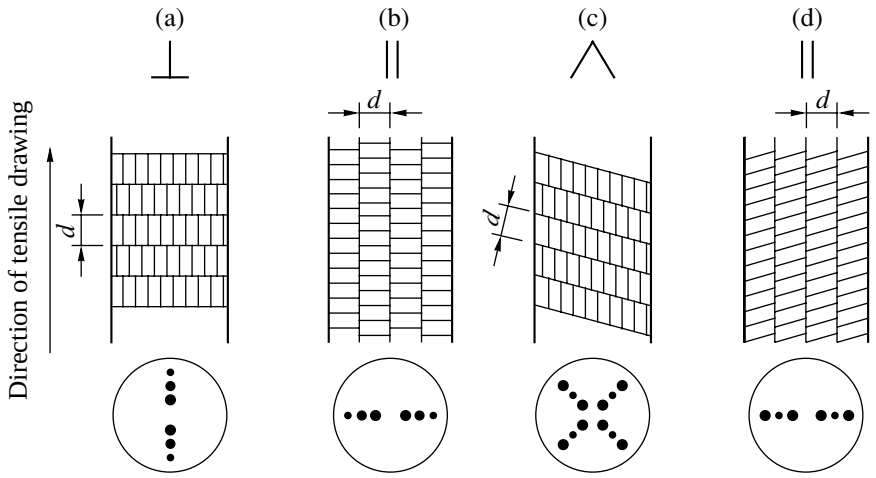

Fig. 11. Layer orientation of (a, b) HE and CA and (c, d) carboxylic acids in the pores of polymer matrices and the arrangement of the corresponding X-ray reflections in the X-ray patterns.

served when either ionic or molecular crystals are introduced into the solvent-crazed polymer matrices.

Even though the orientation of low-molecular-mass compounds in the structure of crazes is seen in all cases, the mode of their orientation depends on the nature of the polymer–low-molecular-mass compound pair. In [22–29], numerous nanocomposites based on various solvent-crazed polymers and incorporated long-chain fatty alcohols, hydrocarbons, and acids have been studied. The crystallization of such compounds is accompanied by the formation of the ordered layers; hence, the interpretation of the corresponding X-ray patterns becomes much easier. The analysis of X-ray patterns shows that a set of pointlike meridional, equatorial, or diagonal reflections may be attributed to the X-ray scattering from the oriented layered planes [27]. Figure 11 presents the schematic representation of the packing of asymmetric molecules in the oriented pores of crazes and the corresponding X-ray reflections.

Normal and parallel orientation of the layered planes of the low-molecular-mass compounds relative to the direction of the tensile drawing of polymers are shown as $\perp$ and $\parallel$, respectively. The inclined order of the layered planes of *n*-carboxylic acids is shown as $\wedge$. Table 2 lists the interplanar distances and the character of orientation of low-molecular-mass compounds in the pores of various solvent-crazed polymers. For comparison, the corresponding data for the same compounds in the free state are presented.

As follows from Table 2, all the above low-molecular-mass substances appear to be oriented upon their crystallization in the polymer matrices. For the linear hydrocarbon, HE, and CA, the layers are oriented perpendicular or parallel to the direction of tensile drawing (along pores) of the polymer (Figs. 11a, 11b, 11d). In addition to the parallel orientation, long-chain acids also show an inclined orientation of crystalline layers (Fig. 11c).

Table 2. Orientation and phase composition of low-molecular-mass compounds in solvent-crazed polymer matrices

Low-molecular-mass compound	Polymer matrix	Orientation	Interplanar distance $d \times 10$, nm	
			in polymer	in free state*
HE	HDPE	⊥	28.8	
	PTFE	⊥	28.6	
	PP	⊥	28.7	
	PET	⊥	28.8	
	PA-6	⊥	28.8	28.65(*A*)
	PC	∥	28.5	28.92(*R*)
	PVC	∥	28.6	
CA	HDPE	⊥	45.5	
	PTFE	⊥	45.4	37.37(γ)
	PET	⊥	45.4	43.83(α)
	PA-6	⊥	45.4	44.9(β)
	PC	∥	45.4	
Undecanoic acid	HDPE	Λ	26.1	25.68(*C*')
	PTFE	∥	25.9	30.16(*A*')
	PC	∥	26.1	
Dodecanoic acid	HDPE	Λ	27.7	
	PP	Λ, ∥	27.7	31.2(*A*)
	PET	Λ, ∥	27.7	27.42(*C*)
	PC	∥	27.7	
TDA	HDPE	Λ	30.1	
	PTFE	Λ	29.8	
	PP	Λ, ∥	30.0	
	PET	Λ, ∥	30.1	
	PA-6	Λ	29.7	35.35(*A*')
	PC	∥	29.7	30.0(*C*')
	PVC	∥	29.8	
	PMMA	∥	29.8	
Pentadecancoic acid	HDPE	Λ	35.5	
	PP	Λ, ∥	35.7	40.2(*A*')
	PET	Λ, ∥	35.6	35.8(*B*')
	PC	∥	35.8	34.4(*C*')

* The corresponding structural modification of the component is given in brackets.

The orientation of low-molecular-mass compounds upon their crystallization in narrow (~10 nm) asymmetric pores of solvent-crazed polymer matrices is primarily controlled by a high thermodynamic stability of the ordered state as compared with that at an arbitrary arrangement. Upon the ordering of the crystallites of the low-molecular-mass compound in crazes, intercrystallite surface energy is minimum. The character of the orientation of low-molecular-mass compounds in polymer matrices is controlled by the minimum free energy of the surface component at the polymer–low-molecular-mass compound boundary. Therefore, each mode of the interaction of crystalline planes depends on the orientation and is characterized by its characteristic value of surface energy.

As was shown in [29, 30], there is a common reason which controls the parameters of the crystalline lattice of the low-molecular-mass compound in the polymer matrix. This reason concerns the presence of inner stresses in solvent-crazed polymer samples. It is important to note that, depending on the level and direction of inner stresses, the character of the deformation of the crystalline lattice of the low-molecular-mass compound is changed.

The orienting effect of the highly developed structure of crazes has an influence not only on the crystallization of ordinary low-molecular-mass compounds. This effect is also seen for the phase transitions in LC compounds. For example, phase transitions of *n*-butoxybenzylidene aminobenzonitrile in the crazes of various polymers were studied in [31]. As was shown, this compound also appears to be oriented in the narrow pores of the solvent-crazed polymers. Such an orientation is well detected by the IR dichroism.

Therefore, the crystalline and LC compounds introduced into the porous structure of the solvent-crazed polymer matrices are oriented with a high level of ordering which may be reversibly changed upon phase transitions.

Indirect Introduction of Low-molecular-mass Compounds into the Structure of Crazes

As was mentioned above, only the limited range of low-molecular-mass compounds can be introduced into the volume of crazes via the direct method. Evidently, the direct method is unable to provide the introduction of substances, which are insoluble in AAM, as well as high-melting substances at temperatures below the glass transition temperature (the melting temperature) of the deformed polymer. Nevertheless, the above polymer-based compositions containing metals, semiconductors, ferroelectrics, and other target additives present an evident interest from the practical viewpoint. Therefore, new approaches were developed to the preparation of nanocomposites via the chemical reactions of corresponding initial compounds directly in the polymer matrix (in situ reactions). Actually, in this case, the microscopic pores in the craze structure may be used as "microreactors" for the synthesis and stabilization of nanophases with a required level of dispersion and a given morphology. The development of nanometric voids makes it possible to utilize them as "microreactors" for various chemical reactions (reduction, exchange, etc.). This approach to the preparation of nanocomposites offers a solution to various fundamental problems concerning the stabilization of nanophases due to a limiting effect of pore walls and a high level of dispersion of thermodynamically incompatible components at the nanometric scale.

The pioneering attempt to conduct the chemical reaction in situ in the structure of the solvent-crazed polymer was described in [19]. That reaction presented a classical photographic process carried out in situ in the structure of the solvent-crazed PET. To this end, the PET film was stretched in an alcohol-containing aqueous solution of potassium iodide. As a result of such tensile drawing, 25 wt % KI was introduced into the polymer. Then, the as-crazed film was placed into the alcohol-containing aqueous solution of silver nitrate. As a result, the crystals of silver iodide were precipitated in the polymer structure. Then, the as-prepared sample was kept in a solution of a standard photographic developer. Upon such a treatment, silver iodide decomposed to a metallic silver. All stages of this process were controlled by the method of X-ray analysis. This process is characterized by a gradual disorientation of the low-molecular-mass component upon in situ reactions. For example, at the first stage, the crystallization of KI is accompanied by the formation of a well-defined orientation, whereas, at the second stage, silver iodide appears to be poorly oriented; at the final stage, the precipitated silver is completely isotropic.

The applicability of the above method of introducing metals into the craze structure is rather limited from the viewpoint of the loading of the craze volume with the low-molecular-mass component. Actually, as the concentration of an inorganic compound in AAM increases, the content of the low-molecular-mass compound in the porous structure of crazes after the solvent evaporation increases [32]. Nevertheless, it is quite evident that this approach does not allow a complete loading of the porous polymer, as it takes place upon the tensile drawing of the polymer in the melt of the low-molecular-mass compound. Even for highly soluble substances such as KI in alcohol-containing aqueous solutions, the content of the inorganic component in the sample does not exceed 30–50 wt % [32]. Figure 12 demonstrates the SEM image of the solvent-crazed PET sample with a tensile strain of 100%; as is seen, the sample shows a well-pronounced open porous structure. Then, the sample was placed into the saturated alcohol-containing aqueous solution of KI and kept there for a week. Evidently, upon such a prolonged treatment, AAM in the porous sample is replaced by a KI-containing solution. Upon a further drying, the PET film containing 47 wt % KI was prepared. Potassium

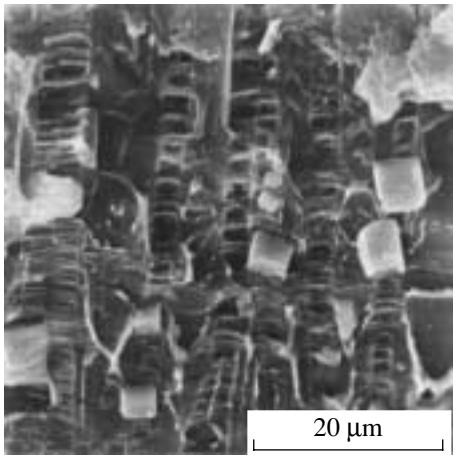

Fig. 12. SEM image of the solvent-crazed PET sample with a tensile strain of 100% after staying in the saturated KI solution.

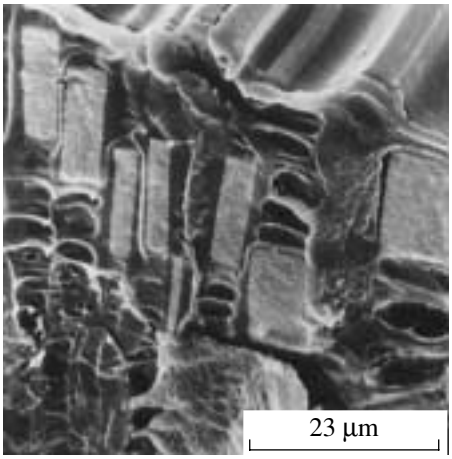

Fig. 13. SEM image of the solvent-crazed PET sample with a tensile strain of 100% after the introduction of AgCl via the countercurrent diffusion.

iodide is precipitated from the saturated solution in craze pores as multiple fine crystals with dimensions of ~2–3 μm, and the crystals are randomly distributed in the pores. The dimensions of such small-sized crystals are not uniform, and this reflects rather random character of their precipitation from the solution. Figure 12 vividly shows that, even though the craze structure is filled with the saturated KI solution, most crazes appear to be free of the low-molecular-mass component.

At the same time, the level of the polymer porosity developed upon its tensile drawing in AAM is known to be rather high. The tensile drawing of glassy polymers in the presence of liquid media proceeds so that the changes in the geometrical dimensions of the deformed sample are primarily provided by the development of porosity when the contributions from other modes of plastic deformation are negligibly small. A trivial estimation allows one to conclude that the complete loading of pores in the solvent-crazed sample with a tensile strain of 100% by the low-molecular-mass compound with a specific weight of 3 g/cm^3 should provide a weight gain of 300 wt % with respect to the weight of the initial polymer matrix.

To overcome the above disagreement and to achieve a high level of loading of the porous structure of the solvent-crazed polymer with an inorganic compound, the method of countercurrent diffusion has been applied [33]. This method of the introduction of low-molecular-mass compounds is different from the above approach. In this case, the solvent-crazed polymer film, that is, the polymer film with an open-porous structure, is placed in the dialysis cell as a membrane separating the neighboring cell compartments containing the solutions of components which are able to react with each other. Low-molecular-mass compounds diffuse toward each other and react directly in the pore volume of the membrane and the chemical reaction takes place in the pores; as a result, the porous structure of the solvent-crazed polymers appears to be efficiently loaded as was shown in [18, 32].

Let us illustrate the above approach with the classical photographic process used in [18]. To this end, the solvent-crazed PET sample was placed into the dialysis cell between the compartments containing alcohol-containing aqueous solutions of $AgNO_3$, from one side, and NaCl, from the other side. After staying in the dialysis cell for one day, the sample was released, rinsed with water, and dried; the as-prepared sample was studied by the SEM method.

Figure 13 shows the SEM image of the solvent-crazed PET film containing AgCl. As is well seen, the precipitation of the low-molecular-mass component is dramatically different from the above process. As follows from Fig. 13, at the center of each craze, one may observe only one crystal of AgCl with a height of ~15 μm; the width of this crystal is equal to a distance between the craze walls. Hence, this approach makes it possible to achieve an efficient loading of the craze volume with the low-molecular-mass inorganic compound. The as-prepared nanocomposition contains appreciable amounts of the highly disperse inorganic compound.

Now, let us conduct the photographic process in the polymer matrix to its end, that is, to the decomposition of AgCl and the precipitation of the metallic silver. To this end, the PET sample with the structure as shown in Fig. 13 was allowed to stay in the standard developer for 2 days. Then, the sample was dried and examined by the SEM method. The resultant SEM images are presented in Fig. 14.

As is seen, upon the treatment of AgCl by the developer, the fine crystals of the metallic silver are precipitated in the volume of crazes. Such crystals are characterized by a more loosened structure as compared with that of the initial AgCl crystals. At the same time, the

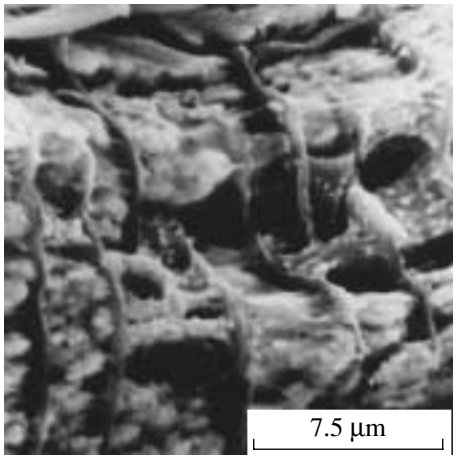

Fig. 14. SEM image of the solvent-crazed PET sample with a tensile strain of 100% after the introduction of AgCl via the countercurrent diffusion and the subsequent treatment by the photographic developer.

analysis of the decomposition of AgCl allows one to clarify the problem concerning the interaction of the growing crystal with the fibrillar craze structure. As follows from Fig. 14, fine silver crystals are located on individual craze fibrils and, in some cases, a specific beadlike structure is formed. This observation suggests that the craze fibrils are involved in the crystalline structure of AgCl (Fig. 13) rather than expelled from it.

Further, numerous studies were devoted to the preparation of various nanocomposites based on different polymers (PP, PE, PA-6, etc.) and metals and metal oxides via the method of countercurrent diffusion [34–41]. In particular, metal-containing polymers were obtained by the countercurrent diffusion of the salts of corresponding metals and reducing agents such as lithium borohydride. As was found, the above procedure shows a universal character and allows the preparation of various nanocomposites. Such nanocomposites may be used as conductors and semiconductors which can be processed as films; the resultant materials are characterized by high mechanical properties which are typical of the initial polymer matrices. The as-prepared composites exhibit various morphological forms. This approach permits one not only to control the total content of the low-molecular-mass disperse phase, its compactness, and the level of dispersion but also to govern its position and arrangement in the polymer phase. Figure 15 schematically shows some possible modes for the location of the low-molecular-phase in the polymer film. Evidently, all the above-mentioned factors are important for the resultant macroscopic properties of the as-prepared nanocomposites (for example, electric conductivity, dielectric permittivity, mechanical characteristics, etc.).

In addition to the above methods, let us discuss another universal approach of metal precipitation from metal compounds via electrolysis. This approach has been applied in [42] for the electrolytic preparation of metal-containing polymer blends based on solvent-crazed polymers. The procedure was the following. The solvent-crazed polymer film was placed onto a graphite electrode in a special electrochemical cell filled with the metal salt solution. The controlled voltage was generated using the second electrode which was also immersed in the solution. As the cathode was covered with a thin porous polymer film, the metal precipitation took place in the pore volume of the polymer matrix. In this way, various solvent-crazed polymer matrices (PVC, PET, HDPE, PP, etc.) were loaded with different metals (Cu, Ni, Fe, Co, Ag, etc.).

The amount of the precipitated metal in the polymer matrix may be controlled by varying the time of electrochemical metal reduction or the porosity of the initial polymer sample. Depending on the mode of solvent crazing [43–46], metallic particles may either be located in the individual narrow zones, crazes, or may produce a highly disperse and continuous phase in the polymer matrix. For example, Fig. 16 presents the SEM images of the solvent-crazed PET samples before and after their treatment in the electrochemical cell. As is seen, this approach allows one to fill the porous structure of crazes from the top to bottom of the film. As in the method of the countercurrent diffusion, the metal involved in the craze volume is not monolithic but is

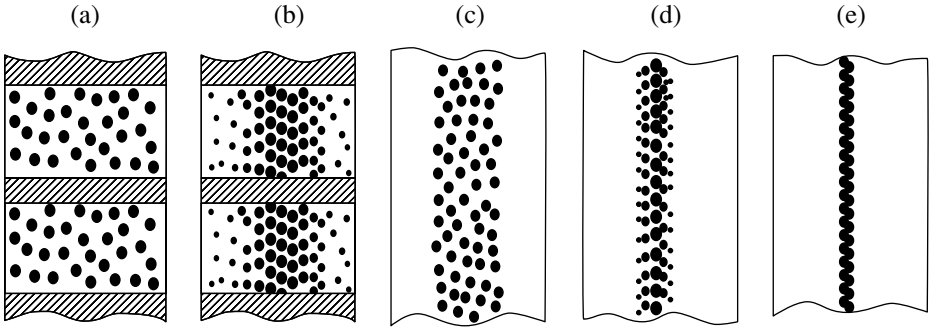

Fig. 15. Schematic representation of various types of the introduction of the low-molecular-mass component into the solvent-crazed polymer matrices via the countercurrent diffusion. The comments are given in text.

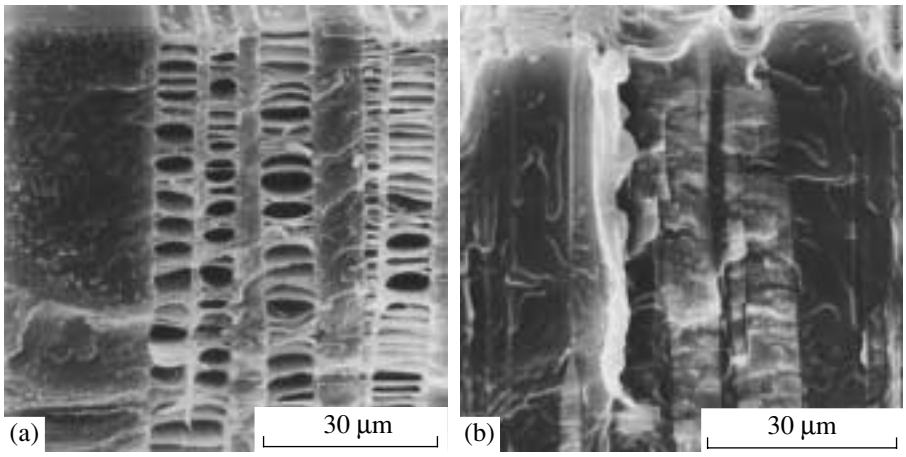

Fig. 16. SEM image of the solvent-crazed PET sample (a) before and (b) after the introduction of metallic copper via electrolytic precipitation.

dispersed in the polymer matrix. As was mentioned above, the pore dimensions, which control the size of the metallic phase, are equal to tens–hundreds of angstroms.

Therefore, the above evidence proves the feasibility of the loading of the porous matrix of the solvent-crazed polymer by almost any target additives in the highly disperse state. The amount of the introduced additive may be more than 300 wt % with respect to the weight of the unfilled polymer matrix. The preparation of such compositions opens a new avenue for the development of new types of complex polymer-based materials.

The metallic filler in the craze volume is not monolithic, but occurs in the highly disperse state in the porous polymer matrix. The diameter of pores, as measured by the method of liquid permeability, is 5–10 nm. The dimensions of metal crystallites in the porous matrix, as follows from the X-ray data, range from 12 to 20 nm.

TECHNOLOGICAL ASPECTS OF THE PREPARATION OF MULTICOMPONENT POLYMER MATERIALS BASED ON SOLVENT-CRAZED POLYMERS

The introduction of various low-molecular-mass additives into polymers presents an important technological problem because, in practice, raw polymers without target additives are not used. In this connection, solvent crazing may be considered as a universal means for the introduction of modifying additives into polymer films and fibers. Let us illustrate this statement and consider a well-known process of dyeing of textile fibers. As is known [47], "dyeing consists of a spontaneous transfer of the dyestuff from the solution to the fiber until an equilibrium is attained. The rate of dyeing and the concentration of the dyestuff in fibers are controlled by the laws of the activated diffusion and soprtion." In the case of a hydrophobic (polyester) fiber, some additional technological tricks are used: "Initially, the fiber is imbibed with a slightly thickened disperse suspension, dried, and heated at 200–210°C (thermosol process) or the fiber is exposed to trichloroethylene vapors (vapokol process)" [47]. Evidently, here, a uniform introduction of the dye in the cross section area of the fiber presents a key problem.

In this context, let us consider some specific features of solvent crazing in the presence of bicomponent liquid media. It is important to mention that, upon solvent crazing, the resultant polymer is characterized not only by the porous structure but also by a well-developed interfacial surface because the dimensions of structural elements in crazes (craze fibrils) are equal to tens–hundreds of angstroms. Solids with a well-developed interfacial surface are referred to as sorbents. Actually, solvent-crazed polymers appear to be nonspecific porous sorbents [48–50]. The very fact of adsorption presents an undoubtedly fascinating phenomenon as it directly proves the presence of the well-developed interfacial surface in the solvent-crazed polymers. In this case, one should also mention that the sorptional experiments provide an opportunity to assess the parameters of the porous structure of solvent-crazed polymers and to characterize their evolution upon tensile drawing in the presence of AAM. To this end, various sorbates with different molecular dimensions are used [48–50].

Figure 17 shows the results of the related sorptional studies as performed for the two sorbates as the weight gain (sorption) plotted against the tensile strain of solvent-crazed polymers. Actually, this evidence allows the characterization of the surface accessibility of the pores in the solvent-crazed samples for sorbing molecules with different dimensions. As is well seen, for the sorbing agent with minimum molecular dimensions (molecular sizes of ~5.4 Å), the as-formed pores are accessible for iodine molecules within the whole range of tensile strains. At low tensile strains of solvent-

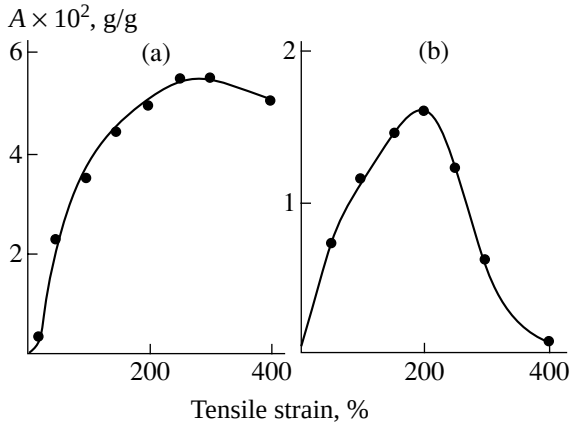

Fig. 17. Sorption of (a) iodine and (b) Rhodamine B vs. the tensile strain of the solvent-crazed PET samples (AAM is propanol). *A* stands for adsorption (weight gain).

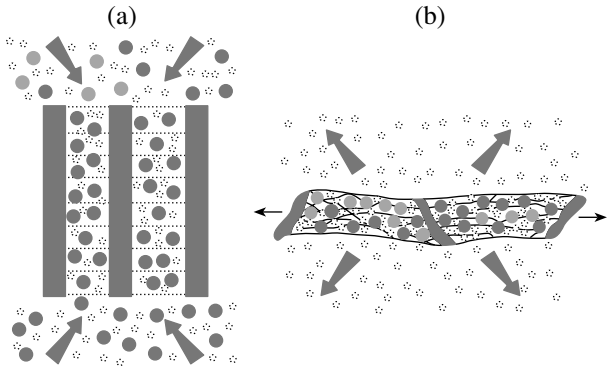

Fig. 18. Schematic representation of structural rearrangements taking place upon the tensile drawing of the polymer via the mechanism of solvent crazing in the bicomponent liquid medium. The arrows show the direction of mass transfer of the low-molecular-mass component at the different stages of solvent crazing.

crazed samples, the sorption of iodine increases because, upon solvent crazing, the interfacial surface area of the polymer increases. Starting at a tensile strain of ~150% (for PET), structural collapse takes place, and this process is accompanied by a marked decrease in the interfacial surface area of the sample [1]. The collapse of the porous structure is also observed in the corresponding sorption curves when the gain in weight levels off with increasing the tensile strain of the solvent-crazed polymer. As the molecular dimensions of the sorbate are increased to 17.5 Å (for organic dye Rhodamine B), the curves describing the weight gain plotted against the tensile strain of the solvent-crazed samples appear to be somewhat different. As is well seen, at tensile strains above ~150%, the sorption of Rhodamine B steadily decreases and tends to zero. Obviously, this decrease in sorption is related to the fact that the molecular dimensions of the sorbate become comparable to the pore dimensions; in this connection, the sorbate molecules are unable to penetrate the volume of crazes.

The analysis of the sorptional data enables one to conclude that, upon solvent crazing, the development of the as-formed porous polymer structure proceeds so that, at early stages of tensile drawing, the pores are large and, hence, accessible both for the small-sized molecules of AAM and bulky molecules of the target additive. At the final stages of solvent crazing, the pore dimensions dramatically decrease; as a result, a certain fraction of the solvent is expelled to the surrounding, and the big-sized molecules of the modifying additive appear to be encapsulated in the porous structure of the polymer sample. Upon a continuous tensile drawing of the polymer in the presence of AAM, the as-formed porous structure gradually passes all the above-mentioned stages of solvent crazing. On the whole, the interaction of the polymer with the solution of the low-molecular-mass additive in AAM may be presented as follows (Fig. 18) [51]. At the early stages of the tensile drawing of the polymer in the presence of the solution of the modifying additive in AAM (Fig. 18a), the as-developed porous structure is continuously filled with the surrounding liquid medium. The stage of the porous structure collapse proceeds so that the big-sized molecules of the modifying additive appear to be entrapped by the collapsing craze structure (Fig. 18b), and the pure AAM is expelled into the surrounding medium (a specific mode of syneresis which is accompanied by osmotic phenomena [52]).

The principal difference between solvent crazing and the above traditional approach [47] is the following. The traditional method is based on a spontaneous transfer of the molecules of the modifying additive to the polymer via diffusion. According to the definition by Rusanov [53], solvent crazing provides “a forced” delivery of the modifying additive dissolved in AAM to a continuously developing nanoporous polymer structure. Hence, this is not surprising that the amount of the as-introduced additive may be much higher than the concentration of the same additive but introduced via an equilibrium sorption from the same solvent [1].

The above results allow the phenomenon of solvent crazing to be regarded as a universal means for the introduction of various modifying additives to polymers. This approach is based on the quite unorthodox mechanisms of delivery and immobilization of modifying additives in the polymer structure. In this case, the additive is delivered not by diffusion but via a far more fast mode of transfer through a viscous flow. To immobilize (to fix) the additive in the structure of a polymer fiber, the polymer and low-molecular-mass component do not necessarily have to contain active functional groups which are capable of any mutual interaction. The immobilization of the additive in the polymer structure is provided by the mechanical entrapment of the low-molecular-mass component when the molecu-

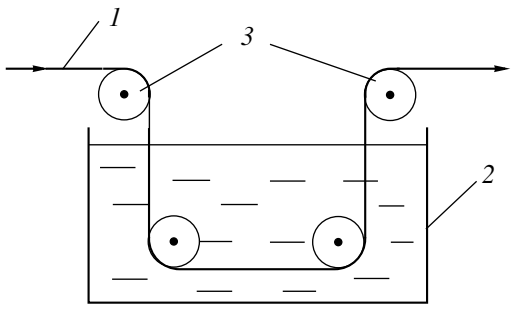

Fig. 19. Schematic representation of the unit for orientational drawing for the modification of polymer films and fibers via solvent crazing: *1* is the polymer film or fiber, *2* is the bath filled with the active liquid medium (possibly, containing the dissolved additive), and *3* are feed and draw rolls.

lar dimensions of the additive are comparable to the pore dimensions in the polymer structure. Taking into account this reasoning, the range of the target additives may be unlimitedly widened. For example, solvent crazing makes it possible to color such hydrophobic polymer as PP by water-soluble vat dyestuff.

As an important feature of the preparation of the compositions based on solvent-crazed polymers, let us mention the fact that the solvent crazing of polymers is a certain mode of inelastic plastic deformation of polymers. This deformation serves as the basis for the technological process of orientational drawing of polymers, which is widely used in the traditional processing of polymers fibers and films. Evidently, such an important stage as orientational drawing is implemented in an accomplished technological solution. Presently, in industry, various high-strain rate machines are used, and orientational drawing of films and fibers is performed under a continuous technological regime. In principle, the modification of polymers via solvent crazing implies that the stage of orientational drawing of polymer films and fibers may be coupled to the stage of the introduction of modifying additives. To this end, the orientational drawing of polymers in the solution of the modifying additive in AAM should be performed in such a way that the traditional technological scheme should be complemented by a rather trivial unit as shown in Fig. 19. In this connection, numerous and successful attempts [54, 55] have been made to implement the process of solvent crazing under a continuous regime. In other words, the technological concept of solvent crazing allows the preparation of nanocomposites as polymer films and fibers with good mechanical characteristics, on one hand, and various valuable properties (electric conductivity, flame retardancy, electrostatic properties, etc.) as imparted by the target additives, on the other hand. Let us emphasize that such nanocompositions may be prepared on an existing technological equipment under a continuous regime at high strain rates, which are typical of the modern industrial production of polymer films and fibers.

REFERENCES

1. Volynskii, A.L. and Bakeev, N.F., *Solvent Crazing in Polymers*, Amsterdam: Elsevier, 1995.
2. Yarysheva, L.M., Lukovkin, G.M., Volynskii, A.L., and Bakeev, N.F., *Uspekhi kolloidnoi khimii i fiziko-khimicheskoi mekhaniki. Sb. Nauchn. Tr.* (Progress in Colloid Chemistry and Physicochemical Mechanics), Shchukin, E.D., Ed., Moscow: Nauka, 1992.
3. Sinevich, E.A., Ogorodov, R.P., and Bakeev, N.F., *Dokl. Akad. Nauk SSSR*, 1973, vol. 212, no. 3, p. 1383.
4. Volynskii, A.L., Aleskerov, A.G., and Bakeev, N.F., *Vysokomol. Soedin., Ser. B*, 1977, vol. 19, no. 3, p. 218.
5. Volynskii, A.L., Aleskerov, A.G., Grokhovskaya, T.E., and Bakeev, N.F., *Vysokomol. Soedin., Ser. A*, 1976, vol. 18, no. 9, p. 2114.
6. Volynskii, A.L., Loginov, V.S., and Bakeev, N.F., *Vysokomol. Soedin., Ser. B*, 1981, vol. 23, no. 4, p. 314.
7. Yarysheva, L.M., Shamolina, T.A., Arzhakova, O.V., Mironova, A.A., Gerasimov, V.I., Volynskii, A.L., and Bakeev, N.F., *Polymer Science, Ser. A*, 1998, vol. 40, no. 6, p. 562.
8. Volynskii, A.L., Arzhakova, O.V., Yarysheva, L.M., and Bakeev, N.F., *Vysokomol. Soedin., Ser. A*, 1989, vol. 31, no. 12, p. 2673.
9. Yarysheva, L.M., Volynskii, A.L., and Bakeev, N.F., *Polymer Science, Ser. B*, 1993, vol. 35, no. 7, p. 1000.
10. Volynskii, A.L. and Bakeev, N.F., *Vysokomol. Soedin., Ser. A*, 1975, vol. 17, no. 7, p. 1610.
11. Volynskii, A.L., Gerasimov, V.I., and Bakeev, N.F., *Vysokomol. Soedin., Ser. A*, 1975, vol. 17, no. 11, p. 2461.
12. Volynskii, A.L., Kozlova, O.V., and Bakeev, N.F., *Vysokomol. Soedin., Ser. A*, 1986, vol. 28, no. 10, p. 2230.
13. Volynskii, A.L., Shelekhin, A.B., Bekman, I.N., and Bakeev, N.F., *Vysokomol. Soedin., Ser. A*, 1988, vol. 30, no. 8, p. 1731.
14. Volynskii, A.L., Shitov, N.A., Yarysheva, L.M., Ukolova, E.M., Lukovkin, G.M., Kozlov, P.V., and Bakeev, N.F., *Vysokomol. Soedin., Ser. A*, 1986, vol. 28, no. 1, p. 178.
15. Volynskii, A.L., Arzhakov, M.S., Karachevtseva, I.S., and Bakeev, N.F., *Polymer Science, Ser. A*, 1994, vol. 36, no. 1, p. 70.
16. Yarysheva, L.M., Karachevtseva, I.S., Volynskii, A.L., and Bakeev, N.F., *Polymer Science, Ser. A*, 1995, vol. 37, no. 10, p. 1044.
17. Kalinina, O. and Kumacheva, E., *Macromolecules*, 2001, vol. 34, no. 18, p. 6380.
18. Volynskii, A.L., Grokhovskaya, T.E., Shitov, N.A., and Bakeev, N.F., *Vysokomol. Soedin., Ser. B*, 1980, vol. 22, no. 7, p. 483.
19. Volynskii, A.L., Shitov, N.A., Chegolya, A.S., and Bakeev, N.F., *Vysokomol. Soedin., Ser. B*, 1983, vol. 25, no. 6, p. 393.

20. Volynskii, A.L., Grokhovskaya, T.E., Lukovkin, G.M., Godovskii, Yu.K., and Bakeev, N.F., *Vysokomol. Soedin., Ser. A*, 1984, vol. 26, no. 7, p. 1456.
21. Kitaigorodskii, A.I., *Molekulyarnye kristally* (Molecular Crystals), Moscow: Nauka, 1971.
22. Moskvina, M.A., Volkov, A.V., Grokhovskaya, T.E., Volynskii, A.L., and Bakeev, N.F., *Vysokomol. Soedin., Ser. A*, 1984, vol. 26, no. 11, p. 2369.
23. Moskvina, M.A., Volkov, A.V., Volynskii, A.L., and Bakeev, N.F., *Vysokomol. Soedin., Ser. A*, 1984, vol. 26, no. 7, p. 1531.
24. Moskvina, M.A., Volkov, A.V., Volynskii, A.L., and Bakeev, N.F., *Vysokomol. Soedin., Ser. A*, 1985, vol. 27, no. 8, p. 1731.
25. Moskvina, M.A., Volkov, A.V., Volynskii, A.L., and Bakeev, N.F., *Vysokomol. Soedin., Ser. A*, 1985, vol. 27, no. 12, p. 2562.
26. Volkov, A.V., Moskvina, M.A., Volynskii, A.L., and Bakeev, N.F., *Vysokomol. Soedin., Ser. A*, 1987, vol. 29, no. 7, p. 1447.
27. Moskvina, M.A., Volkov, A.V., Grokhovskaya, T.E., Volynskii, A.L., and Bakeev, N.F., *Vysokomol. Soedin., Ser. A*, 1987, vol. 29, no. 10, p. 2115.
28. Moskvina, M.A., Volkov, A.V., Efimov, A.V., Volynskii, A.L., and Bakeev, N.F., *Vysokomol. Soedin., Ser. B*, 1988, vol. 30, no. 10, p. 737.
29. Volkov, A.V., Moskvina, M.A., Arzhakova, O.V., Volynskii, A.L., and Bakeev, N.F., *J. Therm. Anal.*, 1992, vol. 38, p. 1311.
30. Volynskii, A.L., Moskvina, M.A., Volkov, A.V., and Bakeev, N.F., *Polymer Science, Ser. A*, 1997, vol. 39, no. 11, p. 1237.
31. Moskvina, M.A., Volkov, A.V., Volynskii, A.L., and Bakeev, N.F., *Vysokomol. Soedin., Ser. A*, 1989, vol. 31, no. 1, p. 160.
32. Volynskii, A.L., Grokhovskaya, T.E., Shitov, N.A., and Bakeev, N.F., *Vysokomol. Soedin., Ser. A*, 1982, vol. 24, no. 6, p. 1266.
33. Volynskii, A.L., Yarysheva, L.M., Arzhakova, O.V., and Bakeev, N.F., *Vysokomol. Soedin., Ser. A*, 1991, vol. 33, no. 2, p. 418.
34. Moskvina, M.A., Volkov, A.V., Zanegin, V.D., Volynskii, A.L., and Bakeev, N.F., *Vysokomol. Soedin., Ser. B*, 1990, vol. 32, no. 12, p. 933.
35. Stakhanova, S.V., Nikonorova, N.I., Zanegin, V.D., Lukovkin, G.M., Volynskii, A.L., and Bakeev, N.F., *Polymer Science*, 1992, vol. 34, no. 2, p. 175.
36. Stakhanova, S.V., Nikonorova, N.I., Lukovkin, G.M., Volynskii, A.L., and Bakeev, N.F., *Vysokomol. Soedin., Ser. B*, 1992, vol. 33, no. 7, p. 28.
37. Stakhanova, S.V., Trofimchuk, E.S., Nikonorova, N.I., Rebrov, A.V., Ozerin, A.N., Volynskii, A.L., and Bakeev, N.F., *Polymer Science, Ser. A*, 1997, vol. 39, no. 2, p. 229.
38. Stakhanova, S.V., Nikonorova, N.I., Volynskii, A.L., and Bakeev, N.F, *Polymer Science, Ser. A*, 1997, vol. 39, no. 2, p. 224.
39. Nikonorova, N.I., Stakhanova, S.V., Volynskii, A.L., and Bakeev, N.F., *Polymer Science, Ser. A*, 1997, vol. 39, no. 8, p. 882.
40. Nikonorova, N.I., Stakhanova, S.V., Chmutin, I.A., Trofimchuk, E.S., Chernavskii, P.A., Volynskii, A.L., Ponomarenko, A.T., and Bakeev, N.F., *Polymer Science, Ser. B*, 1998, vol. 40, no. 3, p. 75.
41. Nikonorova, N.I., Trofimchuk, E.S., Semenova, E.V., Volynskii, A.L., and Bakeev, N.F., *Polymer Science, Ser. A*, 2000, vol. 42, no. 8, p. 855.
42. Volynskii, A.L., Yarysheva, L.M., Lukovkin, G.M., and Bakeev, N.F., *Polymer Science*, 1992, vol. 34, no. 6, p. 476.
43. Volynskii, A.L., Yarysheva, L.M., Ukolova, E.M., Kozlova, O.V., Vagina, T.M., Kechek'yan, A.S., Kozlov, P.V., and Bakeev, N.F., *Vysokomol. Soedin., Ser. A*, 1987, vol. 29, no. 12, p. 2614.
44. Volynskii, A.L., Yarysheva, L.M., Shmatok, E.A., Ukolova, E.M., Arzhakova, O.V., Lukovkin, G.M., and Bakeev, N.F., *Dokl. Akad. Nauk SSSR*, 1990, vol. 310, no. 2, p. 380.
45. Yarysheva, L.M., Shmatok, E.A., Ukolova, E.M., Lukovkin, G.M., Volynskii, A.L., Kozlov, P.V., and Bakeev, N.F., *Vysokomol. Soedin., Ser. B*, 1990, vol. 32, no. 7, p. 529.
46. Volynskii, A.L., Shmatok, E.A., Ukolova, E.M., Arzhakova, O.V., Yarysheva, L.M., Lukovkin, G.M., and Bakeev, N.F., *Vysokomol. Soedin., Ser. A*, 1991, vol. 33, no. 5, p. 1004.
47. Mel'nikov, B.N., *Entsiklopediya polimerov* (Encyclopedia of Polymers), Moscow: Sovetskaya Entsiklopediya, 1972, vol. 1, p. 1135.
48. Volynskii, A.L., Loginov, V.S., Platé, N.A., and Bakeev, N.F., *Vysokomol. Soedin., Ser. A*, 1980, vol. 22, no. 12, p. 2727.
49. Volynskii, A.L., Loginov, V.S., Platé, N.A., and Bakeev, N.F., *Vysokomol. Soedin., Ser. A*, 1981, vol. 23, no. 4, p. 805.
50. Volynskii, A.L., Loginov, V.S., and Bakeev, N.F., *Vysokomol. Soedin., Ser. A*, 1981, vol. 23, no. 5, p. 1059.
51. Volynskii, A.L., Loginov, V.S., and Bakeev, N.F., *Vysokomol. Soedin., Ser. A*, 1981, vol. 23, no. 5, p. 1031.
52. Volynskii, A.L., Loginov, V.S., and Bakeev, N.F., *Vysokomol. Soedin., Ser. A*, 1981, vol. 23, no. 3, p. 567.
53. Rusanov, A.I., Abstracts of Papers, *3 Mezhdunarodnaya konf. "Khimiya vysokoorganizovannykh veshchestv i nauchnye osnovy nanotekhnologii"* (3 Int. Conf. "Chemistry of High-Organized Substances and Fundamentals of Nanotechnology"), St. Petersburg, 2001, p. 16.
54. Guthrie, R.T., Hirshman, J.L., Littman, S., Suckman, E.J., and Ravenscraft, P.H., US Patent 4001367, 1977.
55. Bakeev, N.P., Lukovkin, G.M., Marcus, I., Mikouchev, A.E., Shitov, A.N., Vanissum, E.B., and Volynskii, A.L., US Patent 5516473, 1996.